

REPORT DOCUMENTATION PAGE

Form Approved
OMB No. 0704-0188

Public reporting burden for this collection of information is estimated to average 1 hour per response, including the time for reviewing instructions, searching existing data sources, gathering and maintaining the data needed, and completing and reviewing this collection of information. Send comments regarding this burden estimate or any other aspect of this collection of information, including suggestions for reducing this burden to Department of Defense, Washington Headquarters Services, Directorate for Information Operations and Reports (0704-0188), 1215 Jefferson Davis Highway, Suite 1204, Arlington, VA 22202-4302. Respondents should be aware that notwithstanding any other provision of law, no person shall be subject to any penalty for failing to comply with a collection of information if it does not display a currently valid OMB control number. PLEASE DO NOT RETURN YOUR FORM TO THE ABOVE ADDRESS.

1. REPORT DATE (DD-MM-YYYY)

24-10-2005

2. REPORT TYPE

Research

3. DATES COVERED (From - To)

Aug 2004 - Sept 2005

The Microwave Behavior of an Anisotropic Negative Index Media

5a. CONTRACT NUMBER

5b. GRANT NUMBER

5c. PROGRAM ELEMENT NUMBER

6. AUTHOR(S)

J. S. Derov, B. W. Turchinets*, E. E. Crisman**,
A. J. Drehman and S. R. Best

5d. PROJECT NUMBER

2305

5e. TASK NUMBER

HA

5f. WORK UNIT NUMBER

02

7. PERFORMING ORGANIZATION NAME(S) AND ADDRESS(ES)

Source code 437890

AFRL/SNHA

80 Scott Dr.

Hanscom AFB 01731-2909

* contractor for CNS Inc.

702 King Farm Blvd, Rockville MD

**contractor for Univ. of RI

Dept. of Chem E, Crawford Hall,

Kingston RI 02881

8. PERFORMING ORGANIZATION REPORT NUMBER

9. SPONSORING / MONITORING AGENCY NAME(S) AND ADDRESS(ES)

-

10. SPONSOR/MONITOR'S ACRONYM(S)

11. SPONSOR/MONITOR'S REPORT NUMBER(S)

AFRL-SN-HS-JA-05-1209

12. DISTRIBUTION / AVAILABILITY STATEMENT

Statement A

DISTRIBUTION STATEMENT A
Approved for Public Release
Distribution Unlimited

13. SUPPLEMENTARY NOTES

PA# ESC 05-1209 Published in Proceedings of the SPIE Optics East 2005, Boston, MA

14. ABSTRACT

Free space microwave measurements are reported for a split ring and post type metamaterial which exhibits negative refraction in a frequency band between 13.5 and 14.5 GHz. Varying azimuthal angles and magnitudes are achieved by changing the polarization of the transmitter and receiver relative to each other and to the anisotropic axes of the material. The amplitude of the cross-polarized transmission has been measured at 50% of the co-polarization level. The maximum amplitude was achieved at a polarization angle of 20° relative to the initial polarization. This polarization conversion indicates there are other losses besides ohmic losses. The polarization rotation effect contributes to apparent transmission loss but could be exploited in applications.

15. SUBJECT TERMS

negative index media, NIM, anisotropic media, left-handed materials, metamaterial, negative index of refraction, polarization

16. SECURITY CLASSIFICATION OF:

a. REPORT

Unclassified

b. ABSTRACT

Unclassified

c. THIS PAGE

Unclassified

17. LIMITATION OF ABSTRACT

UU

18. NUMBER OF PAGES

3

19a. NAME OF RESPONSIBLE PERSON

John Derov

19b. TELEPHONE NUMBER (include area code)

781-377-2638

The microwave behavior of an anisotropic negative index medium

John Derov*, Beverly Turchinetz*, Everett Crisman**, Alvin Drehman* and Steven Best*

* Air Force Research Laboratory, Sensors Directorate, Hanscom AFB, MA

** University of Rhode Island, Chemical Engineering Dept., Kingston, RI

ABSTRACT

Free space microwave measurements are reported for a split ring and post type metamaterial which exhibits negative refraction in a frequency band between 13.5 and 14.5 GHz. Varying azimuthal angles and magnitudes are achieved by changing the polarization of the transmitter and receiver relative to each other and to the anisotropic axes of the material. The amplitude of the cross-polarized transmission has been measured at 50% of the co-polarization level. The maximum amplitude was achieved at a polarization angle of 20° relative to the initial polarization. This polarization conversion indicates there are other losses besides ohmic losses.

Keywords: negative index of refraction, NIM, left-handed, metamaterials, anisotropic

1. INTRODUCTION

The theoretical possibility of alternate propagating solutions to Maxwell's equations by media with simultaneously negative electric permittivity and magnetic permeability was first proposed by Veselago¹ in 1967. He predicted several effects unique to such media, including negative index of refraction. In the usual positive refraction between two media, the refracted ray crosses to the opposite side of the optical normal axis from the incident ray. Negative refraction occurs at the interface between positive and negative index media. The refracted ray is bent to the same side of the normal as the incident ray. Negative index media (NIM) have also been referred to as left-handed, double negative and backward wave media. Veselago's work assumed the medium was homogeneous, isotropic and continuous. The first experimental demonstration of negative index of refraction² used a metamaterial consisting of a periodic array of metallic structures made up of split ring resonators (SRRs) and long narrow metallic posts. This material was not isotropic, and only effectively homogenous or continuous due to its tenth-wavelength cell size, but it displayed negative refraction nonetheless. Because of the material's anisotropy, this first demonstration of negative refraction required a linearly polarized electromagnetic field propagating along an axis, similar to the optical axis of a crystal. The anisotropy of negative index media may be particularly complex. The SRR-post type metamaterial we have measured, which is similar to those reported in the literature, can exhibit positive or negative refraction at the same frequency depending on signal polarization. The negative region has also shown bi-anisotropic³ coupling between electric and magnetic response, which was proposed by Marques et al.⁴

The negative index metamaterial combines two different structures. Long, thin metallic posts simulate electrical plasma producing negative permittivity. Split ring resonators provide the magnetic plasma characteristic producing negative permeability in a frequency band near their self-resonance⁵. The post and ring arrays of the cells were etched on the front and back respectively from copper (1 oz per square foot) on 0.254 mm thick Rogers' 5880 circuit board. The relative permittivity of the circuit board was 2.2 at 10 GHz. The unit cell for the split ring-post structure is shown in Fig. 1. The outer ring is 2.7 mm on a side. The line width of the rings is 0.25 mm, the space between rings is 0.30 mm and the gap in each ring is 0.51 mm across. The post on the back is 0.76 mm wide. The unit cell is stepped in an array with 3.71 mm spacing center to center. The posts are joined top to bottom across adjoining cells to form continuous posts 250 mm long. Then the boards are cut into strips of varying widths and stacked to form either a wedge shaped prism or rectangular slabs. The prism increases in thickness from 6 to 16 cells by one cell for every five strips across the width. This produces a wedge apex angle of 12° . Two slabs were constructed with 6 or 16 unit cells thickness. The width of each prism was 20 cm and the height 25 cm. A prism top view is shown in Fig. 2. The orientation of the boards in the prism is vertical, i.e. out of the page of Fig. 2, and parallel to the normal of the entrance face. The posts on the boards are also vertical. The boards are spaced with 3.2 mm layers of Emerson and Cumings Eccosorb™ PP2 foam, which is essentially transparent to microwaves. To hold its shape each prism or slab was wrapped in Top Flight MonoKote, a thin self-adhesive plastic with very low microwave loss, which is typically used to cover model airplanes.

20060713088

All measurements in this report were performed in free space in an anechoic chamber, with matched square transmit and receive horns measuring 20 cm on a side. Each horn has a 3dB width of 14°. The transmit horn is mounted 3.73 m from the prism. The prisms were placed in a baffle with an aperture 20 cm by 25 cm. The receive horn is mounted on a rotating arm 2.58 m from the prism allowing us to measure the angular distribution of the transmitted signal. The horns are connected to a HP-8530A transceiver to measure the amplitude and phase. A block diagram of the system is shown in Fig. 3. The frequencies of interest are near 14 GHz. Note the transmit and receive distance are both beyond the Fresnel diffraction region or R1, the reactive near field distance, given by

$$R1 = 0.62 \sqrt{\frac{D^2}{\lambda}} \quad (1)$$

For the transmit side, where $D = 28.3$ cm, the maximum (diagonal) linear dimension of the source aperture and $\lambda = 2.14$ cm the free space wavelength at 14 GHz then $R1 = 63.7$ cm. This is approximately one-fourth of the antenna to specimen separation. This distance R1 is the transition region between Fresnel and Fraunhofer diffraction for the aperture and any surface wave interactions with the medium would occur at a distance less than or equal to a wavelength. The far field distance to the Fraunhofer diffraction region where the 14° transmit beam width approximates a plane wave is given by

$$R2 = \frac{2D^2}{\lambda} \quad (2)$$

With D and λ as above, $R2$ is 746.4 cm or approximately twice the distance of the antenna to the target. For our experimental setup the wedge is illuminated by 6° compared to the 14° beam, or less than half. This should minimize the phase front variation. The plane wave approximation is reasonable at the specimen interface.

2. MEASUREMENTS

An initial refraction measurement experiment was performed on the wedge prism to confirm negative refraction of the unit cell design. Because of the anisotropy of the medium, a linearly polarized TEM wave with the electric field vector oriented parallel to the posts and the magnetic field vector normal to the plane of the SRRs in the structure is required to excite negative refraction. This polarization is shown in Fig. 2(a.). The incident beam is normal to the entrance face of the prism and continues into the metamaterial without refracting. The beam strikes the second face at an angle equal to the prism apex angle of 12°, and is refracted there. The refracted angles are assigned negative or positive values according to whether the beam is bent to the same or opposite side of the normal as the incident beam, as labeled in Fig. 2 (a.) and (b.). The index of refraction, n , for the metamaterial is calculated by applying Snell's Law,

$$n \sin(\alpha) = n_0 \sin(\theta_r) \quad (3)$$

where $n_0 = 1$, α is 12° and θ_r is the measured exit angle in air. The measurement at 13.5 GHz shows the refracted angle is -12° corresponding to index n of -1 at that frequency (Fig. 4). Additional measurements were made at 13.5GHz with varying angle of incidence from the normal axis at the initial wedge interface⁶. In this case, refraction occurs at both the entrance and exit faces of the prism. Propagation within the prism is not along the optical axis of the material and the magnetic field is no longer normal to the plane of the SRRs. The measured angles and magnitudes of the exit beam show contradictory results, illustrating the complexities of this anisotropic medium. The measured exit angles fall along the curve predicted by applying Snell's Law at both prism faces as if the medium was indeed isotropic, for entrance angles out to 30° from the normal axis (Fig. 5). The raw data in Fig. 6, however, show that the amplitude for the refracted beam falls off rapidly as the entrance angle changes. This indicates that the split ring resonator is sensitive to the angle of the magnetic field. It also suggests that it will be difficult to develop an isotropic medium from structures of this type.

The dispersion of the medium was determined by measuring the refracted angle of the wedge prism at different frequencies. The index was calculated using Equation (3) and plotted in Fig. 7. The frequency region for which the index is negative is necessarily limited and highly dispersive, as predicted by Veselago. This split ring-post structure exhibits

adjacent frequency bands of negative and positive index. The rate of change of the index in the negative region is noticeably greater than in the positive region.

To improve understanding of the attenuation in the medium, the frequency response of the 6 and 16 unit cell slabs was measured. Use of the slab eliminates the complications of refraction when illuminated normal to the interface. Results are shown in Fig. 8. Recall the frequency for which index n equals -1 for the wedge occurs at 13.5 GHz. This lies along the leading edge of the pass band of the slabs. The insertion loss at 13.5 GHz was -4.92 dB for the 6-cell slab and -16.86 dB for the 16-cell slab. The minimum insertion loss, at 14.1 GHz, was -1.80 dB and -5.60 dB for the 6 and 16-cell slabs respectively. The attenuation coefficients per unit length were calculated using the slab thicknesses. The results from the measurements are 3.22 dB/cm at 13.5 GHz and 1.02 dB/cm at 14.1 GHz. These attenuation numbers represent the total loss in the medium which includes conductive, dielectric, scattering, surface wave and parasitic coupling. To investigate the scattered loss, we want to distinguish the anisotropy due to the one dimensional geometry of the wedges and slabs and the anisotropic nature of the negative index response.

Anisotropic prisms such as we have fabricated are described in the literature as indefinite media⁷. The permittivity and the permeability tensors include both positive and negative values. For instance, the x and y components may equal 1 while the z component may equal -1 . The effect of this anisotropy can be demonstrated with the wedge prism and a TEM wave polarized as shown in Fig. 2 (b.). Both the transmitter and receiver polarization are rotated by 90° from our initial arrangement. The direction of propagation was maintained normal to the entrance face of the wedge prism. The magnetic field is parallel to the substrates, which minimizes coupling to the resonators. The electric field is perpendicular to the posts and nearly unaffected by them, as long as they are thin and sparse. The dielectric substrate does of course have an effect, but the boards are usually less than ten percent of the prism volume, the rest being air. The exit angle measured with this polarization was $+12^\circ$ from the normal, meaning the index of refraction for this polarization is equal to $+1$. The prism therefore has a positive index of refraction of nearly unity at the same frequencies for which the orthogonal polarization has a negative index. Further, the use of intermediate polarizations between the two orthogonal mentioned can split the incident signal into two simultaneous output signals, one negatively refracted and one refracted positively. The angular separation of the two output signals is determined by the prism angle and the negative index of refraction at the particular frequency. The results of angle sweeps at 13.5 GHz for various polarizations are overlaid in Fig. 9. The signal magnitude scales with the angle of polarization rotation. The response is similar to previous reported measurements for a unit cell with two posts⁸.

The cross polarization through the wedge prism was measured at 13.5 GHz with the transmitter vertical (E field parallel to posts) and the receiver horizontal (E field perpendicular to posts). As Fig. 10 shows, the signal peak for the cross-polarization was measured at the same angle, -12° from the normal, and almost 50% the magnitude of the co-polarization case. This rotation is a significant scattering loss mechanism which has been previously neglected. Marques⁴ has modeled the bi-anisotropic property of the SRR, which has an electric dipole moment with both orthogonal and coupled magnetic dipole moments. The existence of the cross polarized field indicates that the SRRs themselves have an electromagnetic asymmetry. These dipole moments may account for the large cross polarization that could arise because the resultant field vector radiated by the SRR is not parallel to the planes of the posts. Since the energy is not absorbed but rotated into another polarization, we define this as scattering loss.

Because the cross-polarization was significant, intermediate angles for the receiver polarization between vertical and horizontal were investigated. The receiver was rotated between 0° and 90° relative to the transmitter in 10° steps and swept about the wedge prism exit face axis. The amplitude of the signal at 13.5 GHz through the prism was maximum when the receiver polarization was rotated 20° from vertical. As shown in Fig. 11, the signal peak power increased from 0.43 to 0.47, or about 10%, by optimizing the receiver polarization

3. CONCLUSIONS

In this investigation we have demonstrated the geometrical anisotropy and bi-anisotropy of the metamaterial by studying its response to linearly polarized fields. It has been shown that the polarization of the incident wave determines whether the refracted response is negative or positive. Measurements of cross polarization through the prism of 50% of the co-polarization transmission magnitude have shown that the scattered loss for this medium is significant and can not be ignored. It should be noted for the polarization measurements that wave guide or guided wave scattering chambers,

which are frequently used to characterize negative index media, have restricted propagation modes limited by their boundary conditions. If the cross polarization we observe in free space does not correspond to an allowed guide mode, the signal would be attenuated. The associated loss would be mistaken for absorption, not scattering, if measured in a guided wave system. The insertion loss through the material of 3.36 dB/cm at 13.5 GHz, where the index n is -1, is therefore composed of both scattering and absorptive losses. The polarization measurements of this SRR-post metamaterial indicate that both the anisotropic and bi-anisotropic behavior require further investigation.

ACKNOWLEDGEMENT

This work was sponsored in part by the Air Force Office of Scientific Research, AFOSR/NE.

REFERENCES

1. V. G. Veselago, "The electrodynamics of substances with simultaneously negative values of ϵ and μ ," Soviet Physics Uspekhi, Vol. 10, pp. 509-514, 1968.
2. R. A. Shelby, D. R. Smith and S. Schultz, "Experimental verification of negative index of refraction," Science, Vol. 292, pp. 77-79, 2001.
3. I. V. Lindell, A. H. Sihvola, S. A. Tretyakov and A. J. Vitanen, *Electromagnetic Waves in Chiral and Bi-isotropic Media*, Artech House, Norwood, Mass., 1994.
4. R. Marques, J. Martel, F. Medina and R. Rafi-El-Idrissi, "Role of bianisotropy in negative permeability and left-handed metamaterials," Phys. Rev. B, Vol. 65, pp. 144440-1 - 144440-6, 2002.
5. J. B. Pendry, A. J. Holden, D. J. Robbins and W. J. Stewart, "Magnetism from conductors and enhanced nonlinear phenomena," IEEE Trans. Microwave Theory Tech., Vol. 47, pp. 2075-2084, 1999.
6. J. S. Derov, B. W. Turchinets, E. E. Crisman, A. J. Drehman, S. R. Best and R. M. Wing, "Free space measurements of negative refraction with varying angles of incidence," IEEE Microwave and Wireless Comp. Lett., Vol. 15, pp.567-569, 2005.
7. D. Smith, P. Kolinko and D. Schurig, "Negative refraction in indefinite media," J. Opt. Soc. Am. B, Vol. 21, No. 5, pp.1032-1043, 2004.
8. J. S. Derov, B. Turchinets, E. E. Crisman, A. J. Drehman and R. Wing, "Negative Index Metamaterial for Selective Angular Separation of Microwaves by Polarization," IEEE AP-S International Symposium and USNC/URSI National Radio Science Meeting, pp.130:1:1-4, Monterey, CA, June 2004.

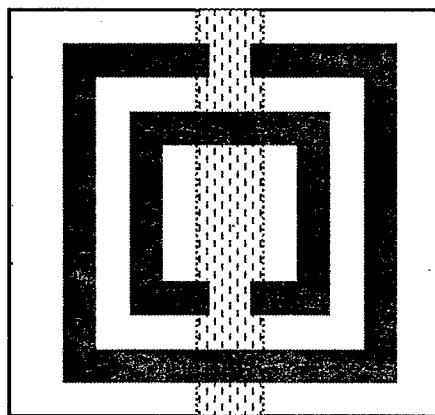


Figure 1. The unit cell with split rings on front and post on back.

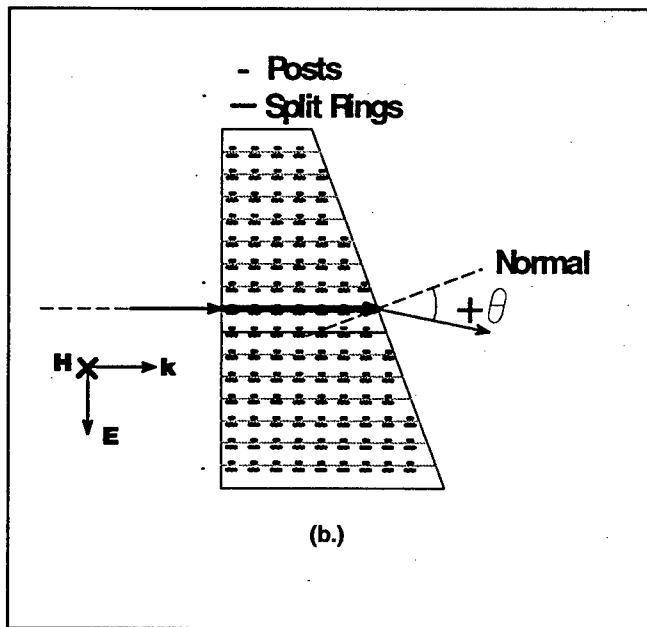
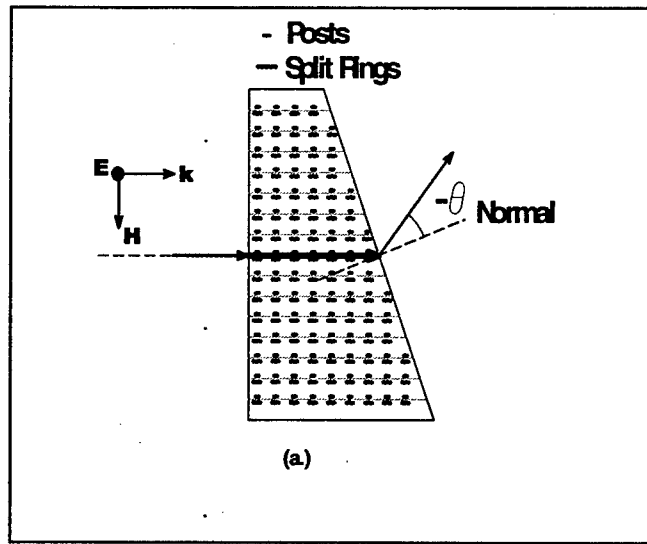


Figure 2. The prism viewed from above showing the effect of polarization on refraction for the same incidence angle. Figure (2a.) shows the field orientation that produces negative refraction through this medium. Figure (2b.) shows the field orientation that produces positive refraction through this medium.

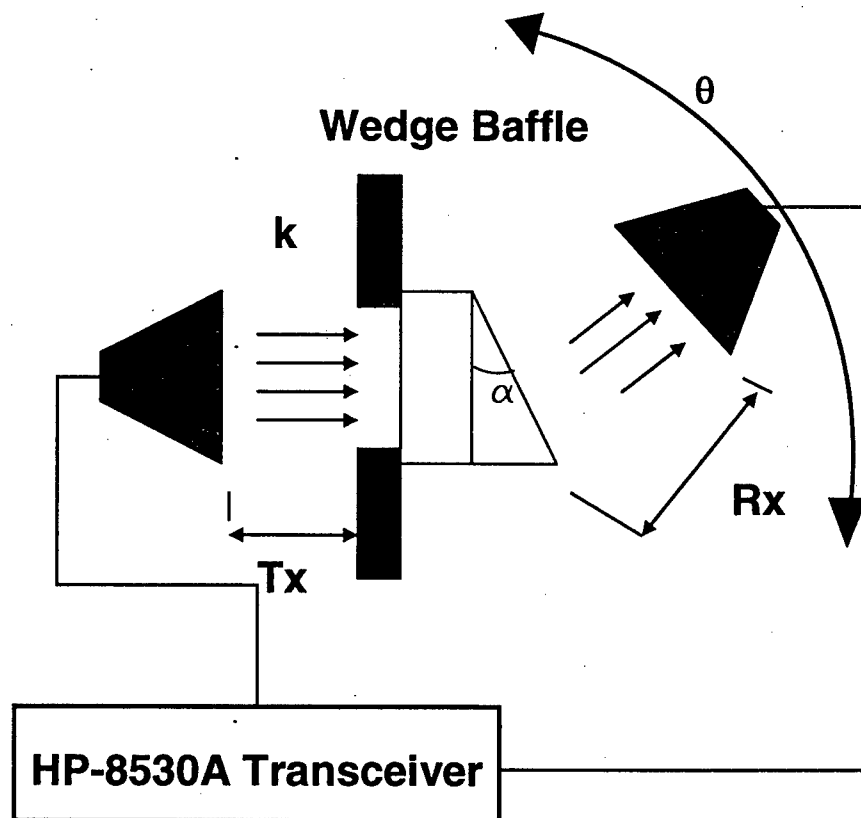


Figure 3. Block diagram of the measurement setup for the refraction and frequency response measurements. Tx and Rx are transmit and receive antenna distances. Diagram not to scale.

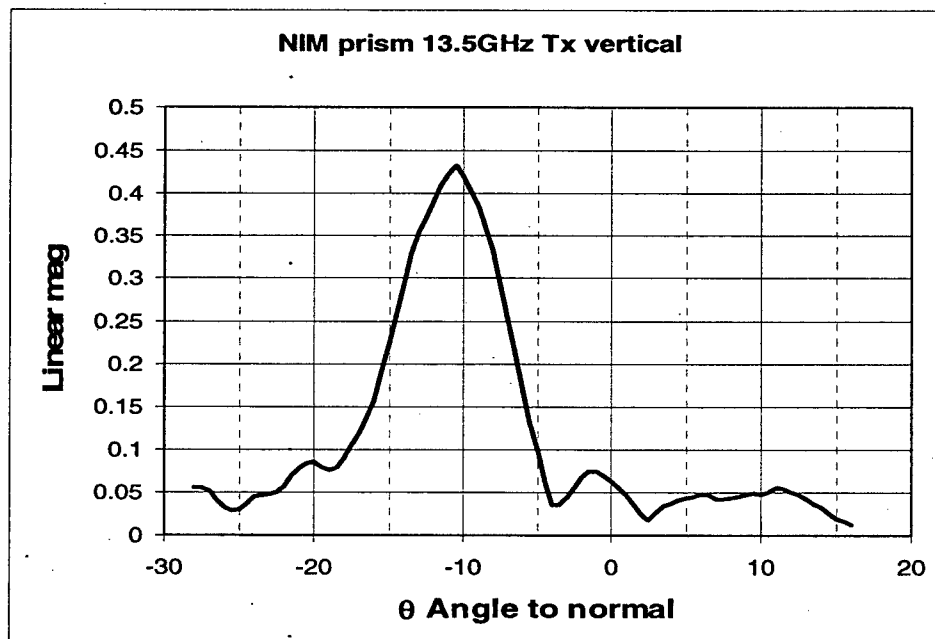


Figure 4. Negative refraction through the 12° wedge.

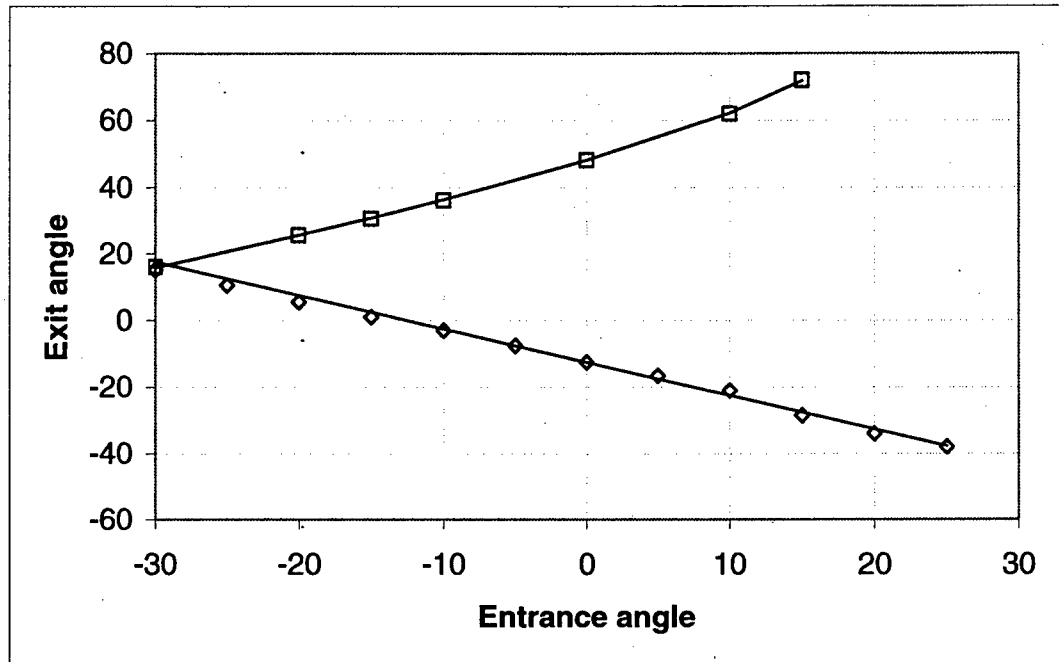


Figure 5. Measured and calculated exit angle with varying entrance angles comparing prisms of tefflon (\square) and metamaterial (\diamond).

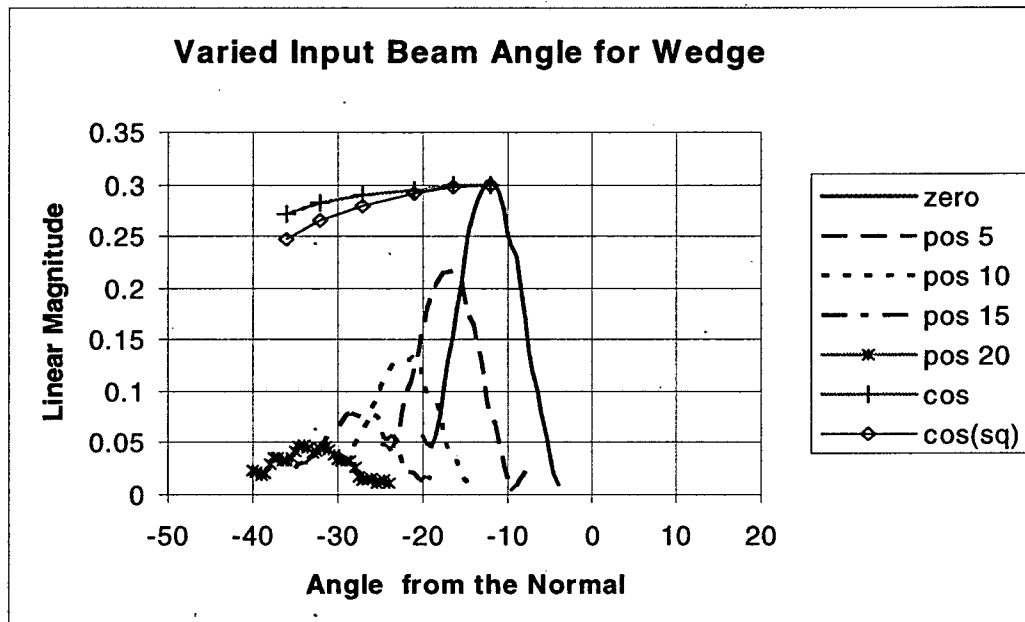


Figure 6. Measured refraction with varying incidence angle. Magnitude rolloff is sharper than \cos or \cos^2 as shown.

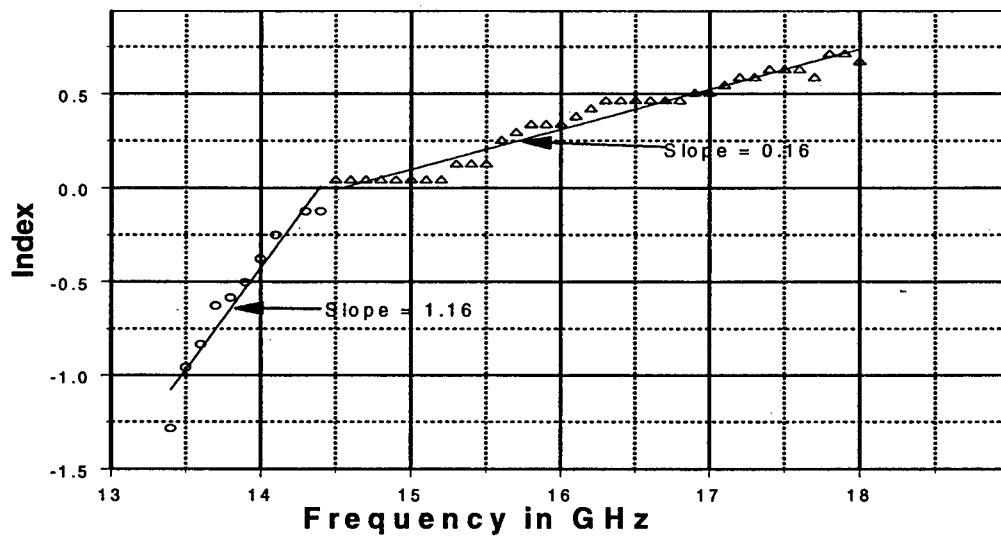


Figure 7. Dispersion from SRR-P prism measurements.

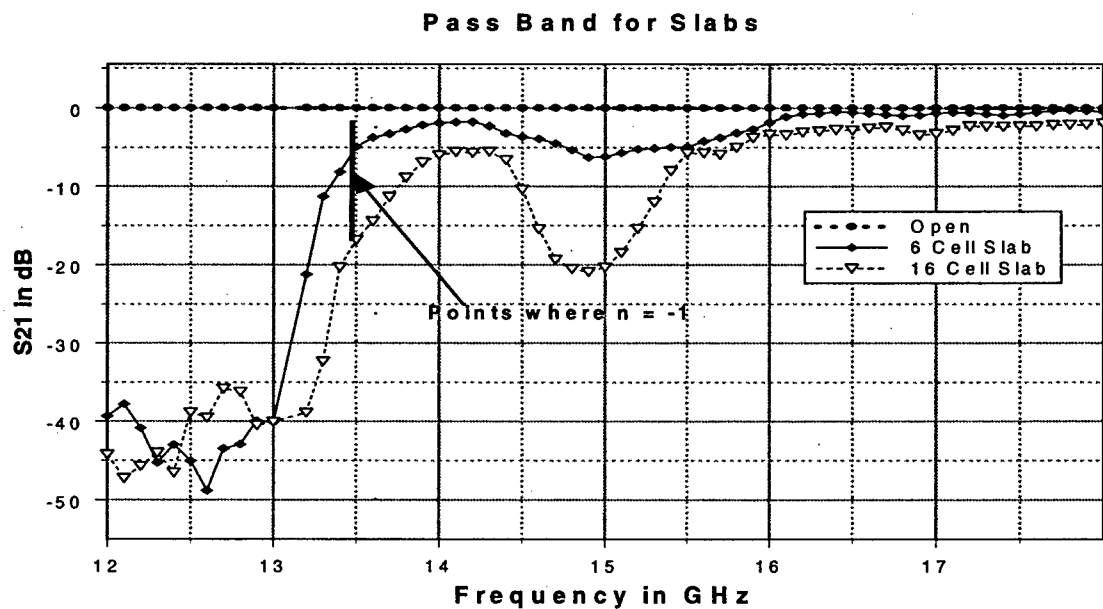


Figure 8. Frequency response through slabs and open baffle.

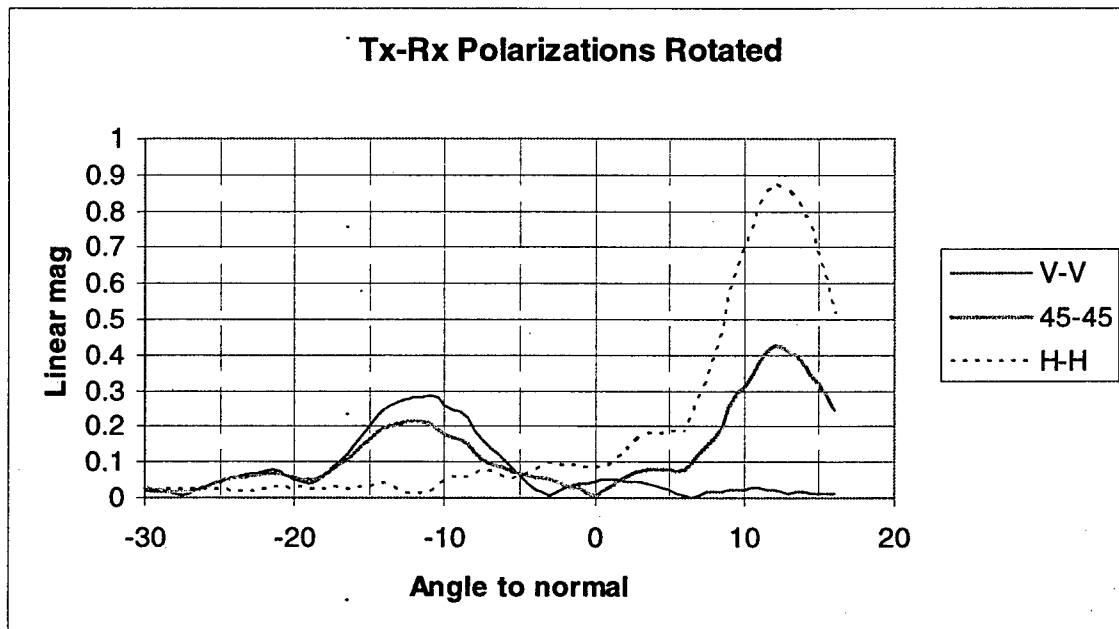


Figure 9. Negative and positive refraction with polarization change of Tx and Rx together.

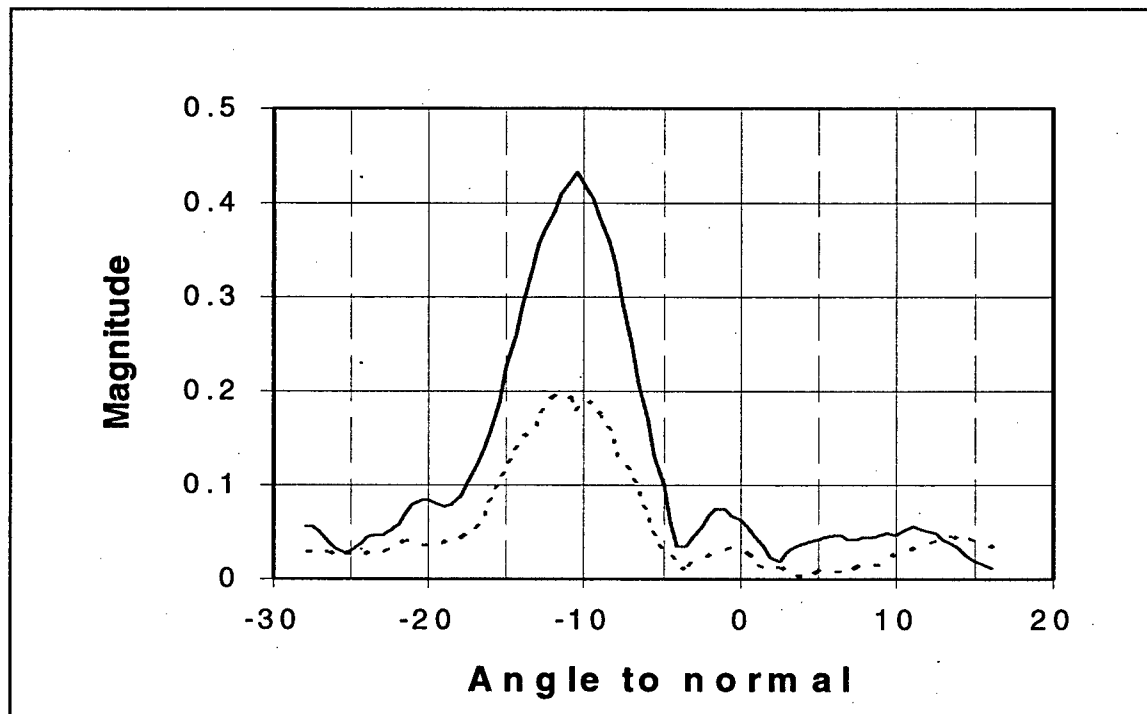


Figure 10. Co (—) and cross (---) polarization through wedge of Rx relative to Tx.

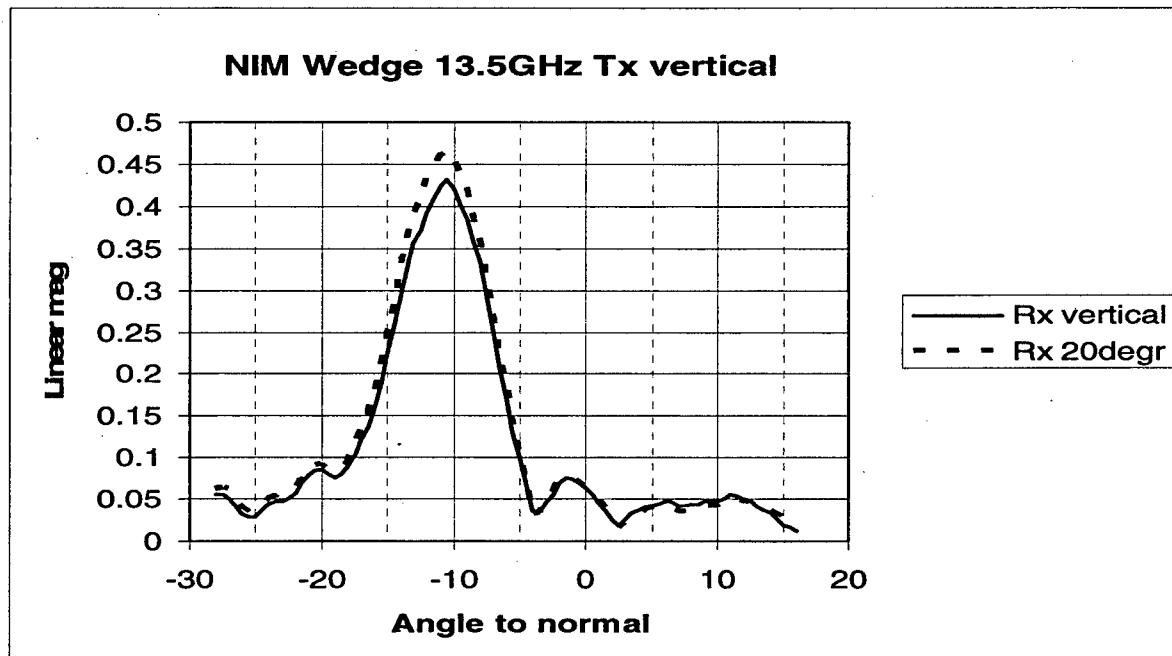


Figure 11. Signal increase for Rx polarization rotated 20° from vertical.